arXiv:cond-mat/0304318v1 [cond-mat.mes-hall] 14 Apr 2003

Effect of bulk inversion asymmetry on the Datta-Das transistor

A. Łusakowski, J. Wróbel, and T. Dietl[*]
Institute of Physics, Polish Academy of Sciences,
al. Lotników 32/46, PL 02-668 Warszawa, Poland
(Dated: February 2, 2008)

A model of the Datta-Das spin field-effect transistor is presented which, in addition to the Rashba interaction, takes into account the influence of bulk inversion asymmetry of zinc-blende semiconductors. In the presence of bulk inversion asymmetry, the conductance is found to depend significantly on the crystallographic orientation of the channel. We determine the channel direction optimal for the observation of the Datta-Das effect in GaAs and InAs-based devices.

PACS numbers: 72.25.Dc, 72.80.Ey, 85.75.Hh, 85.35.-p

Various spin-orbit (SO) effects which are always present in semiconductor quantum structures, are recognized as an important issue in the emerging field of spintronic devices. Already the first proposal of a spin transistor by Datta and Das[1] relied on the SO-induced splitting of the carrier bands in high electron mobility transistors (HEMT). As postulated by Bychkov and Rashba,[2] in such systems, owing to the SO interaction and interfacial electric field $\boldsymbol{E}$ (the structure inversion asymmetry - SIA), the spins of the electrons flowing with the velocity $\boldsymbol{v}$ precess in a magnetic field $\boldsymbol{B}_R \sim \boldsymbol{E} \times \boldsymbol{v}$. To take advantage of this fact, Datta and Das considered a hybrid structure consisting of a ballistic quasi-one-dimensional (1D) wire patterned of a 2D HEMT and of ferromagnetic source and drain ohmic contacts, serving as spin injector and detector, respectively. The contacts were assumed to be magnetized along the current direction and to have 100% spin injection/detection efficiency. The calculated conductance for such a device was found to oscillate as a function of the SO coupling strength α, whose magnitude could be controlled *via* a metal gate located on the top of the structure. Datta and Das showed that in the lowest order in α the oscillations depended on neither 1D sub-band index n nor electron wave vector k.

Since the original proposal of Datta and Das, the operation of their spin field-effect transistor (spin-FET) has been analyzed in much detail. For example, calculations of device conductance not only for small but also for large α were carried out[3] as well as possible effects of electron-electron interactions were analyzed.[4] Furthermore, an important problem of spin injection across the ferromagnet/semiconductor interface was considered from various viewpoints.[5,6,7] However, in addition to the SIA (Rashba) term, owing to the lack of inversion symmetry in bulk materials – there exists the so-called bulk inversion asymmetry (BIA) or Dresselhaus term.[8] It is known that the combined effect of both terms modifies considerably spin properties of zinc-blende heterostructures.[9] Therefore, the SIA and BIA contributions should be considered on equal footing when analyzing the performance of spin devices.[10]

In this work, we consider a ballistic quantum wire patterned of a zinc-blende heterostructure grown along the [001] direction. The Hamiltonian describing the electron motion takes into account both SIA and BIA terms. By a numerical solution of the Schrödinger equation for GaAs- and InAs-based systems, we demonstrate the importance, of hitherto neglected, non-linear terms in the BIA hamiltonian. Moreover, we show that the device performance depends strongly on the wire direction in respect to the crystal axes. This allows us to determine channel orientation corresponding to the largest transconductance for both GaAs and InAs based devices.

In order to model the Datta-Das transistor, we consider an infinite quantum wire that extends in the x direction, which is oriented at an angle of ϕ to the [100] crystal axis. The potential confining electrons in y direction, $V(y)$, is assumed to be parabolic and characterized by the energy difference between consecutive harmonic oscillator levels $\hbar\omega_0$=1 meV in GaAs and $\hbar\omega_0$=3 meV in InAs, respectively. In order to simulate the presence of ferromagnetic electrodes, we assume that in the regions $x < 0$ and $x > L$ the electron spins experience the magnetic field $|B_{\rm out}| = 10^3$ T, which is strong enough to ensure the entire spin polarization. Following Datta and Das we take the vectors $\boldsymbol{B}_{\rm out}$ to point in the x direction and consider the case of their parallel or anti-parallel relative orientations. In the channel region, $0 < x < L$, $B_{\rm out}$ decays adiabatically to zero. For $x \parallel [100]$, the SO Hamiltonian is given by[11]

$$H_{SO} = i\alpha\left(\sigma_y\partial_x - \sigma_x\partial_y\right) + i\gamma\left(\sigma_x\partial_x\left(\partial_y^2 + \langle k_z^2\rangle\right) - \sigma_y\partial_y\left(\langle k_z^2\rangle - \partial_x^2\right)\right), \qquad (1)$$

where σ_x and σ_y are the Pauli matrices. The terms proportional to α and γ corresponds to the SIA and BIA, respectively, whose effect on the band splitting has been thoroughly examined.[12] Here, we estimate the magnitude of α and $\langle k_z^2\rangle$ according to Ref. 11

$$\alpha = \frac{\hbar^2}{2m}\frac{\Delta\left(2E_g + \Delta\right)}{E_g\left(E_g + \Delta\right)\left(3E_g + 2\Delta\right)}\frac{2\pi e^2 N_s}{\kappa}; \qquad (2)$$

---

[*] Address in 2003: Institute of Experimental and Applied Physics, Regensburg University; supported by Alexander von Humbold Foundation

$$\langle k_z^2\rangle = \frac{1}{4}(16.5\pi e^2 m N_s/\kappa\hbar^2)^{1/3}, \qquad (3)$$

which gives values comparable with those obtained from the more refined theories, at least in low Fermi energy limit. In Eq. (2) κ is the static dielectric constant, m is the effective mass, E_g is the energy gap, and Δ is the spin-orbit splitting in the valence band.[13] For example, for typical areal electron density $N_s = 5\times10^{11}$ cm^{-2}, this approach implies α =1.7 meVÅ and 42.0 meVÅ for GaAs- and InAs-based heterostructures, respectively. The BIA parameter γ is equal to 25 eVÅ^3 for GaAs and 130 eVÅ^3 for InAs.[11,14]

By transforming the Hamiltonian (1) to a new coordinate system such that the angle between new and old x axes is ϕ we obtain,

$$\begin{aligned} H_{SO} &= i\alpha\left(\sigma_y\partial_x - \sigma_x\partial_y\right) \\ &-i\gamma\left[\sigma_y\sin(2\phi)\left(\frac{1}{2}\partial_x^2 - \frac{1}{2}\partial_y^2 + \langle k_z^2\rangle\right)\right. \\ &\left. - \sigma_x\cos(2\phi)\left(\partial_y^2 + \langle k_z^2\rangle\right)\right]\partial_x \\ &-i\gamma\left[\sigma_y\cos(2\phi)\left(\partial_x^2 + \langle k_z^2\rangle\right)\right. \\ &\left. + \sigma_x\sin(2\phi)\left(\frac{1}{2}\partial_y^2 - \frac{1}{2}\partial_x^2 + \langle k_z^2\rangle\right)\right]\partial_y. \qquad (4)\end{aligned}$$

We see that only the Dresselhaus (BIA) term changes, while the Rashba (SIA) term remains invariant with respect to the rotations around the z axis.
The full Schrödinger equation for our calculations reads,

$$\begin{aligned}&\left(-\frac{\hbar^2}{2m}\left(\partial_x^2 + \partial_y^2\right) + V(y) + H_{SO}\right. \\ &\left.+\frac{1}{2}g\mu_B\boldsymbol{\sigma}\cdot\boldsymbol{B}_{\rm out}(x)\right)\Psi(x,y) = E_F\Psi(x,y), \qquad (5)\end{aligned}$$

where E_F is the Fermi energy.

To calculate conductance in the non-interacting electron model we employ the recursive Green function method[15] in a form developed in Ref. 16. We expand the spinor wave function $\Psi(x,y)$ into a series

$$\Psi(x,y) = \sum_n \chi_n(x)\psi_n(y), \qquad (6)$$

where $\psi_n(y)$ are the eigenfunctions of one dimensional harmonic oscillator potential

$$\left(-\frac{\hbar^2}{2m}\partial_y^2 + V(y)\right)\psi_n(y) = \epsilon_n\psi_n(y). \qquad (7)$$

By using the orthonormality property of these functions, it is easy to derive a set of differential equations for $\chi_n(x)$.

The problem we encounter is the appearance of third order derivative with respect to x in the term $-i\gamma\sin(2\phi)\partial_x^3\chi_n(x)$, which originates from the BIA part of the Hamiltonian. We replace this term by $i\gamma\sin(2\phi)k_x^2(n)\partial_x\chi_n$ where $k_x^2(n) \equiv \frac{2m}{\hbar^2}\left(E_F - \epsilon_n\right)$ is the wave vector for n'th mode in the absence of spin-orbit coupling. This approximation is justified by the fact that for typical experimental situations, $\gamma k_F^3 << \frac{\hbar^2 k_F^2}{2m}$. Indeed, for GaAs for $k_F \sim 10^8$m^{-1} and $\gamma = 25$ meVÅ^3, $\gamma k_F^3 \sim 4.0\times10^{-24}$ J, which is much smaller than $\frac{\hbar^2 k_F^2}{2m} \sim 8\times10^{-22}$ J. In other words, the spatial changes of the wave function are governed mainly by the $-\frac{\hbar^2}{2m}\partial_x^2$ term in the Hamiltonian. Treating χ_n as the components of a vector $\boldsymbol{\chi}$ we arrive to

$$-\frac{\hbar^2}{2m}R\left(\partial_x^2\boldsymbol{\chi} + 2iQ\partial_x\boldsymbol{\chi}\right) + \left(h - E_F\right)\boldsymbol{\chi} = 0, \qquad (8)$$

where matrix $Q \equiv R^{-1}P$ and

$$R_{nn'} = \delta_{nn'} + i\frac{2m}{\hbar^2}\gamma\left[\sigma_y\cos(2\phi) - \frac{1}{2}\sigma_x\sin(2\phi)\right]D^{(1)}_{nn'}; \qquad (9)$$

$$\begin{aligned} P_{nn'} &= \frac{m}{\hbar^2}\gamma\{\delta_{nn'}\sigma_y\sin(2\phi)[\langle k_z^2\rangle - \frac{1}{2}k_x^2(n)] \\ &-\delta_{nn'}\langle k_z^2\rangle\sigma_x\cos(2\phi) - [\sigma_x\cos(2\phi) \\ &+\frac{1}{2}\sigma_y\sin(2\phi)]D^{(2)}_{nn'}\} - \frac{m}{\hbar^2}\alpha\delta_{nn'}\sigma_y; \qquad (10)\end{aligned}$$

$$\begin{aligned} h_{nn'} &= \left(\epsilon_n + \frac{1}{2}g\mu_B\boldsymbol{\sigma}\cdot\boldsymbol{B}_{\rm out}(x)\right)\delta_{nn'} \\ &-i\gamma\left[\langle k_z^2\rangle\left(\sigma_y\cos(2\phi) + \sigma_x\sin(2\phi)\right)D^{(1)}_{nn'}\right. \\ &\left.+\frac{1}{2}\sigma_x\sin(2\phi)D^{(3)}_{nn'}\right] - i\alpha\sigma_x D^{(1)}_{nn'}, \qquad (11)\end{aligned}$$

and the the matrix $D^{(n)}_{mn} = \langle\chi_m|\partial_y^{(n)}|\chi_n\rangle$. After discretization along x direction (with the lattice constant a) we finally obtain

$$\begin{aligned} &-tV_{x,x+a}\boldsymbol{\chi}(x+a) - tU_{x,x-a}\boldsymbol{\chi}(x-a) + 2tR\boldsymbol{\chi}(x) \\ &-\frac{\hbar^2}{2m}RQ^2\boldsymbol{\chi}(x) + \left(h - E_F\right)\boldsymbol{\chi}(x) = 0, \qquad (12)\end{aligned}$$

where $t = \frac{\hbar^2}{2ma^2}$, $V_{x,x+a} = Re^{iaQ}$, $U_{x,x-a} = Re^{-iaQ}$. This form is appropriate for the conductance calculation.

Before presenting our results we discuss briefly the "linear" approximation to the BIA term. Within this approximation second order derivatives ∂_x^2 and ∂_y^2 are neglected in Eq. (4). On the basis of this linear approximation one can easily understand the influence of the channel crystallographic orientation on the performance of spin-FET. Let us consider a transversal running mode characterized by wave vector k. Following Datta and Das[1] we neglect intermode coupling caused by spin-orbit terms. Then, it is possible to define Rashba and Dresselhaus "magnetic fields" $\boldsymbol{B}_R = \alpha k(0,-1)$ and $\boldsymbol{B}_D = \gamma\langle k_z^2\rangle k(-\cos2\phi, \sin2\phi)$. Their sum $\boldsymbol{B}_{SO} = \boldsymbol{B}_R + \boldsymbol{B}_D$ determines the spin precession frequency. Importantly,

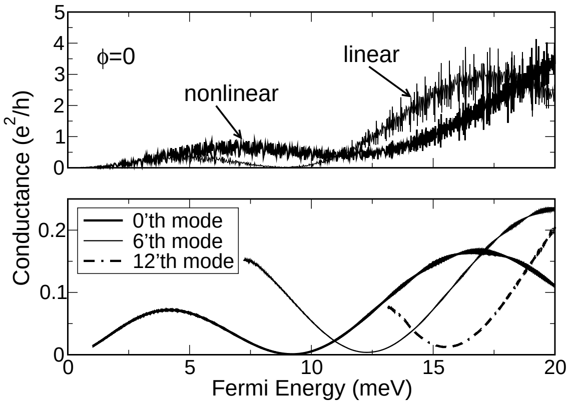

FIG. 1: Source-drain conductance of a GaAs-based device as a function of the Fermi energy for ϕ=0 ([100] channel direction) and anti-parallel electrode magnetizations. Upper panel - comparison of linear and nonlinear cases. Lower panel - partial contributions of three chosen modes to the conductance.

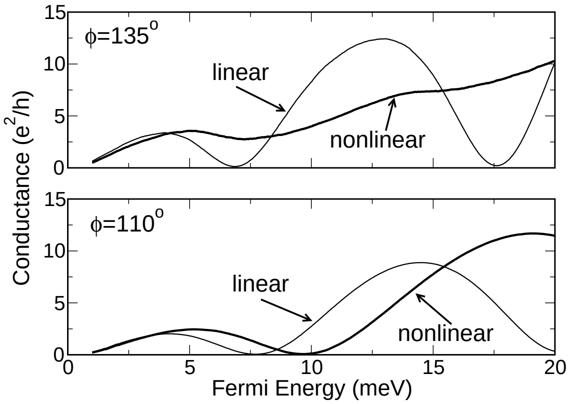

FIG. 2: Source-drain conductance of a GaAs-based device as a function of the Fermi energy for $\phi = 135^\circ$ (upper panel) and for for $\phi = 110^\circ$ (lower panel).

the magnitude and orientation of $\boldsymbol{B}_{SO}$ with respect to the x axis depend on the angle ϕ. That is why the precession frequency varies with the channel crystallographic orientation. It is easy to find out that for $\phi = 135^\circ$, $\boldsymbol{B}_{SO}$ is perpendicular to the x axis, and its length assumes a maximum value. Thus, for the $[\bar{1}10]$ channel orientation, in the linear approximation, the period of the oscillations is the shortest, and thus the Datta-Das effect best visible. These qualitative considerations have been confirmed by our numerical calculations performed in the linear approximation. However, in neither GaAs nor InAs the linear approximation is justified for the experimentally relevant Fermi energy range.

We start the discussion of the full nonlinear model from results for the device oriented along the [100] direction ($\phi = 0$). As shown in the upper panel of Fig. 1, for a given relative magnetization of the contacts, two types of conductance oscillations as a function of the Fermi energy appear: the long-period Datta-Das oscillations and the short-period Fabry-Perot oscillations resulting from interference between transmitted and reflected spin wave functions by the two contacts.[5] In real experiments, the latter are expected to be washed out by thermal broadening and effects of non perfect geometry. Therefore, in the following pictures we show smoothed data obtained by averaging with the Fermi energy window of 1.0 meV. We realize that in the nonlinear case, contributions to the conductance originating from particular modes oscillate with different periods. When the Fermi energy or, equivalently, electron concentration grows, every 1 meV a new mode, with its own period, starts to participate in the transport. We illustrate this effect in the lower panel of Fig. 1, where a partial conductance due to 0th, 6th and 12th mode is depicted. This leads to the disappearance of the conductance minima when the nonlinear terms in the SO Hamiltonian are taken into account, as shown in Fig. 2 (upper panel). By analyzing the conductance for different angles ϕ we have found that the optimal angle for the observation of Datta-Das effect in GaAs is $\phi = 110^\circ$ (see Fig. 2 lower panel).

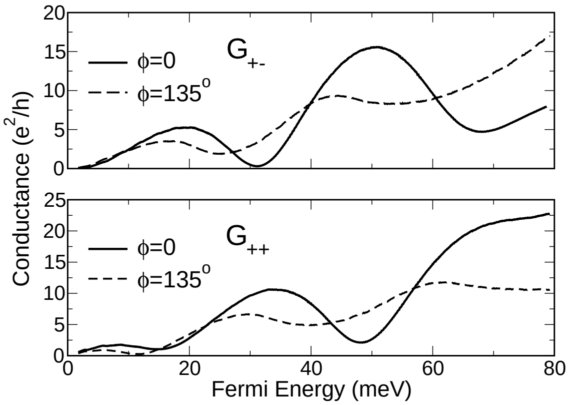

FIG. 3: Source-drain conductance of a InAs-based device as a function of the Fermi energy for $\phi = 0^\circ$ and $\phi = 135^\circ$ for the opposite (upper panel) and parallel (lower panel) source-drain polarizations.

Turning to the InAs-based transistors, we note that different ratios of parameters describing SIA and BIA terms result in a different behavior of the conductance as a function of the transistor direction. For InAs the spin-orbit parameters are about order of magnitude larger, however, the electron mobility in InAs is low comparing to GaAs so the length of the quantum wire have to be shorter, otherwise we cannot assume ballistic transport regime. In calculations we have assumed L=4.0 μm.[17] The results for the optimal angle ϕ=0° are presented in Fig. 3. They are compared to the case ϕ=135° which is the optimal angle determined within the linear approach. In Fig. 3 we show conductance for opposite (upper panel) and parallel (lower panel) source-drain polarizations, respectively.

The angle dependence of conductance for GaAs and

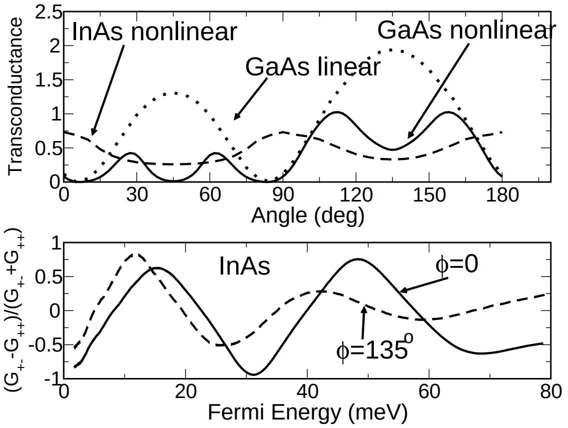

FIG. 4: Upper panel - Transconductance as a function of channel's direction. Lower panel - Relative difference of conductances for opposite and parallel source-drain polarizations.

InAs devices is summarized in the upper panel of Fig. 4, where we plot the transconductance, $|dG/dE_F|$, a quantity of particular experimental interest. The transconductance in Fig. 4 is defined as the absolute value the derivative of conductance with respect to the Fermi energy. For a given angle ϕ, we take into account the energy region, where the conductance decreases. Indeed, a decrease of G is directly connected with the Datta-Das effect while its increases is connected also with the increasing number of modes participating in the transport. In the lower panel of Fig. 4 we present the Fermi energy dependence of another quantity which is also important in the experimental search for the Datta-Das effect,[5,6] $P = (G_{+-} - G_{++})/(G_{+-} + G_{++})$, where G_{++} and G_{+-} are conductances for parallel and opposite source-drain polarizations respectively. Our results imply, therefore, that there is much room for the enhancement of the Datta-Das signal by selecting an appropriate crystallographic orientation of the device.

In conclusion, we have developed a theoretical approach suitable to numerical studies of ballistic electron transport in semiconductor wires taking into account spin-orbit effects. The model has been applied to the Datta-Das spin-FET of zinc-blende semiconductors. There are two main results of our model calculations. First, there is a strong dependence of the transistor conductance on its direction with respect to crystallographic axes. Secondly, our calculations explicitly show the importance of nonlinear terms in BIA Hamiltonian. For particular model of the spin-orbit parameters, Eq. (2) and Eq. (3), we have also determined transistor direction optimal for the observation of the Datta-Das effect, which is $[\bar{1}20]$ and [100] for the GaAs and InSb-based devices, respectively.

The work was supported by the KBN grant PBZ-KBN-044/P03/2001, FENIKS project (EC: G5RD-CT-2001-0535), and Centre of Excellence CELDIS (ICA1-CT-2000-70018) within the 5th Framework Programme of European Commission. The authors thank P. Pfeffer for discussions concerning the role of nonlinear terms in BIA Hamiltonian.

---

[1] S. Datta and B. Das, Appl. Phys. Lett. **56**, 665 (1990).

[2] Yu.L. Bychkov and E.I. Rashba, J. Phys. C **17**, 6093 (1984).

[3] F. Mireles and G. Kirczenow, Phys. Rev. B **64**, 024426 (2001).

[4] A. V. Moroz, K.V. Samokhin, and C.H.W. Barnes, Phys. Rev. Lett. **84**, 4164 (2000); W. Häusler, Phys. Rev. B **63**, 121310 (2001); M. M. Larsen, A. M. Lunde, and K. Flensberg, Phys. Rev. B **66**, 03304 (2002).

[5] T. Matsuyama *et al.*, Phys. Rev. B **65**, 155322 (2002).

[6] G. Meier, T. Matsuyama, and U. Merkt, Phys. Rev. B **65**, 125327 (2002).

[7] P. Mavropoulos, O. Wunnicke, and P.H. Dederichs, Phys. Rev. B **66**, 024416 (2002); L.W. Molemnkamp, G. Shmidt, and G.E.W. Bauer, Phys. Rev. B **64**, 121202(R) (2001).

[8] G. Dresselhaus, Phys. Rev. **100**, 580 (1955).

[9] Y. Ohno *et al.*, Phys. Rev. Lett. **83**, 4196 (1999); N.S. Averkiev and L.E. Golub, Phys. Rev. B **60**, 15582 (1999); W. Knap *et al.*, Phys. Rev. B **53**, 3912 (1996).

[10] J. Schliemann, J.C. Egues, and D. Loss, Phys. Rev. Lett. **90**, 146801 (2003).

[11] F.G. Pikus and G.E. Pikus Phys. Rev. B **51**, 16928 (1995).

[12] P. Pfeffer, Phys. Rev. B **59**, 15902 (1999); P. Pfeffer, Phys. Rev. B **55**, R7359 (1997); L. Wissinger, U. Rosseler, R. Winkler, B. Jusserand, and D. Richards, Phys. Rev. B **58**, 15375 (1998)

[13] For parameters of III-V compounds, see, I. Vurgaftman, J.R. Meyer, and L.R. Ram-Mohan, J. Appl. Phys. **89**, 5815 (2001); D. Bimberg *et al.*, in Numerical Data and Functional Relationships in Science and Technology, edited by O. Madelung, M. Schulz, and W. Weiss, Landolt-Börnstein, New Series, Group III, Vol. 17, Pt. a (Springer, Berlin, 1982).

[14] E. A. D. E. Silva, G. C. LaRocca, and F. Bassani, Phys. Rev. B 50, 8523 (1994).

[15] P.A. Lee and D.S. Fisher, Phys. Rev. Lett. **47**, 882 (1981); A. MacKinnon and B. Kramer, Z. Phys. B **53**, 1 (1983); M. Cieplak, B. R. Bułka, and T. Dietl, Phys. Rev. B **53**, 12337 (1991).

[16] I. V. Zozoulenko, F.A. Maaø, and E.H. Hauge, Phys. Rev. B **53**, 7975 (1996); *ibid*, p. 7987.

[17] J. Eroms *et al.*, Europhys. Lett. **58**, 569 (2002).